Received 8 August 2014
Revised 22 October 2014
Accepted 11 December 2014

Human heart preservation analyses using convective cooling

Abas Abdoli and George S. Dulikravich
Department of Mechanical and Materials Engineering, MAIDROC Laboratory, Florida International University, Miami, Florida, USA
Chandrajit L. Bajaj
Department of Computer Sciences, Computational Visualization Center, Institute of Computational Engineering and Sciences, University of Texas at Austin, Austin, Texas, USA
David F. Stowe
Departments of Anesthesiology and Physiology, Cardiovascular Research Center, Medical College of Wisconsin, Milwaukee, Wisconsin, USA, and
Salik M. Jahania
Department of Surgery, Division of Cardiothoracic Surgery, School of Medicine, Wayne State University, Detroit, Michigan, USA

Abstract

Purpose – Currently, human hearts destined for transplantation can be used for 4.5 hours which is often insufficient to test the heart, the purpose of this paper is to find a compatible recipient and transport the heart to larger distances. Cooling systems with simultaneous internal and external liquid cooling were numerically simulated as a method to extend the usable life of human hearts.

Design/methodology/approach – Coolant was pumped inside major veins and through the cardiac chambers and also between the heart and cooling container walls. In Case 1, two inlets and two outlets on the container walls steadily circulated the coolant. In the Case 2, an additional inlet was specified on the container wall thus creating a steady jet impinging one of the thickest parts of the heart. Laminar internal flow and turbulent external flow were used in both cases. Unsteady periodic inlet velocities at two frequencies were applied in Case 3 and Case 4 that had four inlets and four outlets on walls with turbulent flows used for internal and external circulations.

Findings – Computational results show that the proposed cooling systems are able to reduce the heart temperature from +37°C to almost uniform +5°C within 25 min of cooling, thus reducing its metabolic rate of decay by 95 percent. Calculated combined thermal and hydrodynamic stresses were below the allowable threshold. Unsteady flows did not make any noticeable difference in the speed of cooling and uniformity of temperature field.

Originality/value – This is the pioneering numerical study of conjugate convective cooling schemes capable of cooling organs much faster and more uniformly than currently practiced.

Keywords Conjugate heat transfer, Cryopreservation, Heart cooling, Organ preservation, Thermal stress, Transplantation

Paper type Research paper

International Journal of Numerical Methods for Heat & Fluid Flow
Vol. 25 No. 6, 2015
pp. 1426-1443

0961-5539
DOI 10.1108/HFF-08-2014-0251

The lead author would like to acknowledge the financial support of a Florida International University Dissertation Year Fellowship. The authors also gratefully acknowledge the FIU Instructional and Research Computing Center for providing HPC resources to perform calculations for this project.

Nomenclature

A	contact area between fluid-solid surfaces
CV	coefficient of variation
C_p	specific heat per unit mass
E	Young's modulus of elasticity
f	frequency
$\vec{f}_b$	body force vector per unit volume
G	Lamé's second coefficient
$\vec{g}$	gravitational acceleration
h	enthalpy per unit mass
h_{conv}	convection heat transfer coefficient
I	unit tensor
K_f	thermal conductivity of fluid
K_s	thermal conductivity of solid
p	static pressure
Q_{10}	constant factor
$\dot{q}$	heat source/sink
$\vec{q}_c$	conduction heat transfer rate
q_{conv}	convection heat transfer flux
q_m	cell metabolic rate
q_{m0}	reference cell metabolic rate
$\vec{\dot{q}}_r$	radiation heat transfer flux
SD	standard deviation
T	absolute temperature
T_0	reference absolute temperature
T_{av}	average volumetric temperature
T_f	fluid temperature
T_s	solid Temperature
$\vec{u}$	solid displacement vector
Greek	
α	thermal diffusivity
ε	strain tensor
ε_T	thermal strain tensor
λ	Lamé's first parameter
μ	dynamic viscosity
μ_T	turbulent viscosity
υ	Poisson's ratio
ρ	density
σ	stress tensor
σ_v	von Mises stress
σ'	deviatoric stress tensor
$\underline{\underline{\tau}}$	viscous stress deviator tensor

1. Introduction

Currently, heart preservation time from the moment of harvesting to the moment of surgical implantation is approximately 4.5 hours during which a heart rests in a cold saline bath. This short period of time has to cover all required steps in a heart transplant process including medical tests, finding matching recipients and performing organ transportation, which is the most time consuming step. Therefore, transportation of the donated heart to the best match recipient is currently strongly dependent upon their distance from the heart harvesting site. The Organ Procurement and Transplantation Network's (OPTN report, 2011) defines five concentric geographical zones in the USA for the heart allocation to regulate and facilitate the transplantation process based on the current limitations in heart preservation (Reyes *et al.*, 2008).

In organ preservation, cold preservation is still considered as the best method. Lowering temperature of cells, tissues and organs lowers chemical reaction rates, thus, lowers their metabolic decay rate and keeps them viable for transplantation for longer periods of time. An empirical relation based on experimental evidence, known as "Q_{10} law", states that for every 10°C reduction in tissue temperature there is a corresponding reduction in cell metabolic rate equal to the constant Q_{10}. The law is written as:

$$\frac{q_m}{q_{m0}} = (Q_{10})^{[(T-T_0)/10]} \tag{1}$$

Here, T is temperature in degrees Celsius and q_m is the cell metabolic rate. Values for Q_{10} range from 2.0 to 3.0 and are cited in the physiology literature (Reyes *et al.*, 2008).

For example, assuming the worst situation where $Q_{10} = 2.0$, it can be observed that reducing temperature from +37 to +27°C reduces the metabolic rate by 50 percent. Reducing temperature to +4°C would reduce the metabolic rate in the same scenario by 89.9 percent thus significantly reducing oxygen and glucose consumption and carbon dioxide production (Moore *et al.*, 2011) so that cell damage due to lack of oxygen will be decreased (Polderman and Herold, 2009). Stowe *et al.* (2002) reported that stopping tissue perfusion and cooling isolated guinea pig hearts to +3.4°C for six hours resulted in a return of left ventricular pressure to 81 percent of that before cooling. The conclusion is that cooling of three-dimensional organs should be as fast and as uniform as possible in order to minimize the time when parts of the organ are still at an elevated temperature thus locally experiencing high metabolic rates (Jahania *et al.*, 1999).

In the early attempts at numerical simulations of cooling organs, Dulikravich (1988) demonstrated using boundary element method, in the case of two dimensions, that it is possible to achieve desired cooling rates at any point of the cooled object by varying cooling container wall temperature distribution. In a more realistic numerical simulation, Dennis and Dulikravich (2000) used 3-D spectral finite elements to simulate unsteady temperature and thermal stress evolution during freezing of an idealized canine kidney submerged in gelatin without perfusion. They also demonstrated computationally the optimized time-varying temperatures and heat fluxes to be used on the surface of a spherical freezing container and suggested optimizing the internal perfusion temperature of the organ during the cooling process. Trunk *et al.* (2003) numerically simulated unsteady heat conduction in a human heart partially submerged in a cold liquid and experimentally confirmed (using a porcine heart) that temperature field was highly non-uniform. Sterk and Trobec (2005) used an explicit finite difference method to simulate cooling of a human heart submerged in a cold liquid including thermal buoyancy, but without forced convection. They used Navier-Stokes equations inside the cooling liquid bath, but not inside the heart. In recent studies, Abdoli *et al.* (2014a, b) numerically analyzed a cooling protocol for a realistic human heart which consisted of the internal perfusion with a cold liquid and simultaneous external conduction cooling with gelatin demonstrating remarkably faster and more uniform cooling.

The work presented here shows that uniformity of temperature field during cooling process and the speed of cooling the heart can further be improved by introducing additional cooling jet nozzles strategically positioned on the cooling container inner wall. The ultimate objective of this research is to extend the viability of the transplant heart to at least ten hours. This would provide up to seven hours for air transport, thus enabling heart transplantations anywhere in the North American continent. As part of achieving this goal, the heart should be brought to a just-above tissue freezing temperature as uniformly and as quickly as possible.

2. Thermo-fluid analysis

The different viscosity, specific heat, heat conductivity and density properties of the heart and bathing/pumped liquid require the modeling analysis to have different domains for solids and fluids. Despite the development of other cooling liquids that are superior in certain aspects (Mühlbachera *et al.*, 1999), we have decided to use The University of Wisconsin (UW) solution (Southard and Belzer, 1995) as the cooling liquid to pump through the heart chambers in all numerical simulations. This liquid

was treated as a Newtonian fluid. The equations for conservation of mass and linear momentum for this case have the form:

$$\nabla.\vec{V} = 0 \tag{2}$$

$$\rho\left(\frac{\partial\vec{V}}{\partial t}+\vec{V}\cdot\nabla\vec{V}\right) = -\nabla p+\nabla\cdot\left(\left(\mu+\mu_T\right)\left[\nabla\vec{V}+\nabla\vec{V}^{T}\right]\right) \tag{3}$$

Here, μ is the dynamics viscosity of fluid and μ_T is turbulent viscosity which includes the effect of velocity fluctuations that were calculated from the $k-\varepsilon$ turbulence model. The conservation of energy for incompressible flow in stagnation enthalpy form was used as:

$$\rho\left[\frac{\partial h_o}{\partial t}+\left(\vec{V}\cdot\nabla\right)h_o\right] = \frac{\partial p}{\partial t}+\nabla\cdot\left(\underline{\underline{\tau}}\cdot\vec{V}-\dot{\vec{q}}_c-\dot{\vec{q}}_r\right)+\rho\vec{g}\cdot\vec{V}+\rho\dot{q} \tag{4}$$

where stagnation enthalpy per unit mass is $h_0 = h+\vec{V}^{2}/2$.

The OpenFOAM software platform was used for simulations (OpenCFD Ltd, 2011). OpenFOAM applies the Pressure Implicit with Splitting of Operators algorithm (Ferziger and Peric, 2001; Jasak, 1996) for the pressure-velocity transient problems. This algorithm allows more than one pressure-velocity correction. Another correction can be applied to account for the non-orthogonality of the computational grid. Thermophysical properties of the UW liquid (Arunachalam *et al.*, 2006) and heart muscle tissue (Freitas, 1999) are shown in Table I.

Heart tissue was considered as isotropic solid materials (Ohayon and Chadwick, 1988). For the solid domains, only energy balance without convection was applied.

Next, a conjugate heat transfer analysis was performed by solving the above governing equations for solid and fluid domains. The main benefit of performing the conjugate heat transfer analysis was that interface temperature distributions and heat flux distributions could be captured iteratively and accurately.

The average volumetric temperature and coefficient of variation (CV) of volumetric temperature were used to further investigate the distribution of temperatures during the cooling process. CV was used to indicate temperature non-uniformity inside the heart tissue and was defined as:

$$\mathrm{CV} = \frac{\mathrm{SD}}{T_{ave}} \tag{5}$$

Here:

$$\mathrm{SD} = \sqrt{\frac{1}{N}\sum_{i=1}^{N}(T_i-T_{ave})^2} \text{ and } T_{ave} = \frac{1}{N}(T_1+T_2+\ \ldots\ +T_N) \tag{6}$$

Material	Density, ρ (kg m^{-3})	Specific heat, C (J $kg^{-1}K^{-1}$)	Heat conductivity, k (W $m^{-1}K^{-1}$)	Viscosity, μ (kg $m^{-1}s^{-1}$)
UW solution	1,025	4,180	0.6	0.0037
Heart tissue	1,060	3,716.98	0.586	–

Table I.
Thermophysical properties

where T_i is the local temperature and N is the number of grid cells inside the heart tissue.

3. Domain coupling

The numerical procedures for coupling fluid and solid domains can be classified into two approaches: monolithic (implicit) and explicit (partitioned). In the monolithic method, the governing equations for both the fluid and solid domains are derived based on the same primitive variables. This leads to one single solution matrix for the entire domain (Hou *et al.*, 2012). In contrast, the partitioned approach uses separate solution matrices, separate mesh discretizations and separate numerical algorithms for fluid and solid domains.

In this research, the partitioned coupling method was used to couple solid and fluid domains. A first order implicit Euler scheme was applied for time discretization. Solvers for each domain were placed inside a loop to achieve the coupled convergence through a global iterative process. Multi-region, three-dimensional, unsteady conjugate heat transfer OpenFOAM solver (chtMultiRegionFoam) was applied for simulations. The chtMultiRegionFoam is a parallel solver that has been validated by different researchers (Peltola, 2011).

4. Stress analysis

Stress analysis was performed for the simulated heart during the cooling process. It was assumed that heart tissue is a homogenous and isotropic material (Ohayon and Chadwick, 1988). The main objectives of stress analysis were to investigate thermal stresses and internal shear stresses created by pumping the cold liquid through the heart chambers during the internal cooling process. The pressure inside the resting heart during cooling is less than the diastolic pressure of the beating heart. Because the heart will not be beating and the cooling process will be continuous (constant fluid flow), it is acceptable to assume there would be little deformation of the heart chambers or vessels during the cooling process. The conservation of momentum for a homogeneous solid body element (Hetnarski and Eslami, 2009) can be written as:

$$\rho \frac{\partial^2 \vec{u}}{\partial t^2} - \nabla \cdot \sigma - \vec{f}_b = 0 \tag{7}$$

For a linear elastic solid, stress tensor, σ, can be written as:

$$\sigma = 2G\varepsilon + \lambda tr(\varepsilon)\mathrm{I} \tag{8}$$

where λ and G can be determined by using the following formulas:

$$\lambda = \frac{E\upsilon}{(1+\upsilon)(1-2\upsilon)} \text{ and } G = \frac{E}{2(1+\upsilon)} \tag{9}$$

The combined strain tensor, ε, is defined as:

$$\varepsilon = \frac{1}{2}\left[\nabla \vec{u} + \left(\nabla \vec{u}\right)^{\mathrm{T}}\right] + \alpha_{\mathrm{v}} \Delta T \mathrm{I} \text{ where } \Delta T = T - T_0 \tag{10}$$

Here, α_{v} is the coefficient of thermal expansion, T_0 is the reference temperature and the superscript T denotes the transpose. Combining Equations (7), (8) and (10), the

governing equation for an isotropic, homogenous, solid body with no motion and no external body forces, becomes:

$$\nabla \cdot \left[G\left(\nabla \overrightarrow{u} + \left(\nabla \overrightarrow{u} \right)^{\mathrm{T}} + 2\alpha_{\mathrm{v}} \Delta T \mathrm{I} \right) + \lambda \mathrm{tr}\left(\nabla \overrightarrow{u} + \alpha_{\mathrm{v}} \Delta T \mathrm{I} \right) \right] = 0 \tag{11}$$

The OpenFOAM stress analysis solver (solidDisplacementFoam) was applied for solving the above equation. This solver is a transient, segregated, finite-volume solver for linear-elastic, small-strain deformations. It also includes thermal stresses. The von Mises stress criteria was used to further study the stress field inside the heart during cooling. The von Mises stress is defined as:

$$\sigma_v = \sqrt{\frac{3}{2}\sigma' : \sigma'} \text{ where } \sigma' = \sigma - \frac{\mathrm{tr}(\sigma)}{3} I \tag{12}$$

The required data for mechanical properties of heart were found to be as follows: Young's modulus of elasticity is 80 kPa (Yamada, 1970), ultimate tensile strength is 110 kPa (Yamada, 1970; Park and Lakes, 2007), Poisson's ratio is 0.4 (Amini and Prince, 2001), and coefficient of thermal expansion is 0.0003 (Palmeri and Nightingale, 2004).

5. Cooling container design

For the present analysis, the real human heart geometry developed by Bajaj and Goswami (2008a, b) from 3-D high definition CT-angio scans was used for all simulations. This model does not include coronary arteries. Therefore, only the major veins were used in the heart cooling system. A cooling container of 214 mm in length, 212 mm in width and 282 mm in height, having two coolant inlets and two coolant outlets on its walls was numerically designed (Figure 1) for circulating coolant outside the heart. The two inlets with 15 mm diameter and two outlets with 20 mm diameter were located on opposite corners of the container walls so that they can create strong fluid vortices around the heart and enhance the heat transfer.

For right and left circulation domains inside the heart, two inlets and two outlets were incorporated to pump the coolant through the heart chambers as shown in

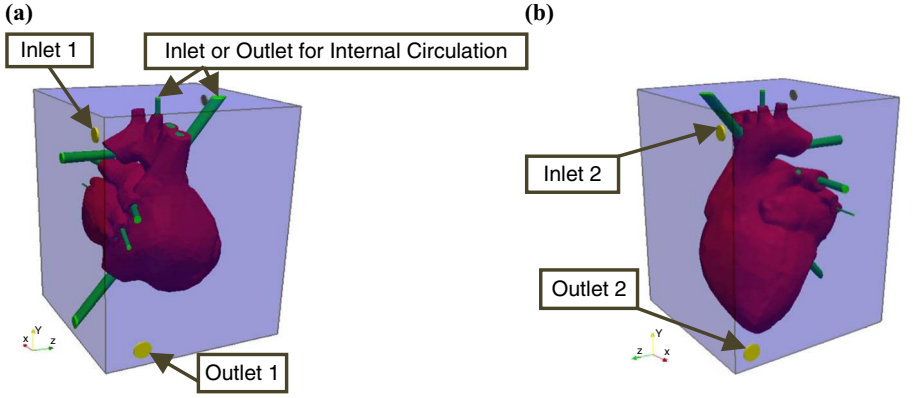

Figure 1. External cooling system

Notes: (a) Inlet 1 and outlet 1 for external cooling; (b) inlet 2 and outlet 2 for external cooling

Figure 2. For the right (pulmonic) heart circulation, the inferior vena cava and superior vena cava are the two flow inlets. One of the right pulmonary arteries and one of the left pulmonary arteries are the two flow outlets (Figure 2(a)) for the right heart. For the left (systemic) heart circulation, one of the left pulmonary veins and one of the right pulmonary veins are the two flow inlets. The aorta with one of its cephalad branches (left common carotid artery) are the two flow outlets (Figure 2(b)) for the left heart. Thus, four inlets and four outlets were used for heart internal circulation.

The UW flow directions inside the heart were the same as those of blood in an intact heart and its circulatory system. At the same time, the UW liquid was pumped inside the cooling container around the heart to remove the heat from outside the heart. The hexahedral mesh was generated for each domain using OpenFOAM snappyHexMesh (OpenCFD, 2011). Figure 3 shows the hexahedral mesh in a sagittal

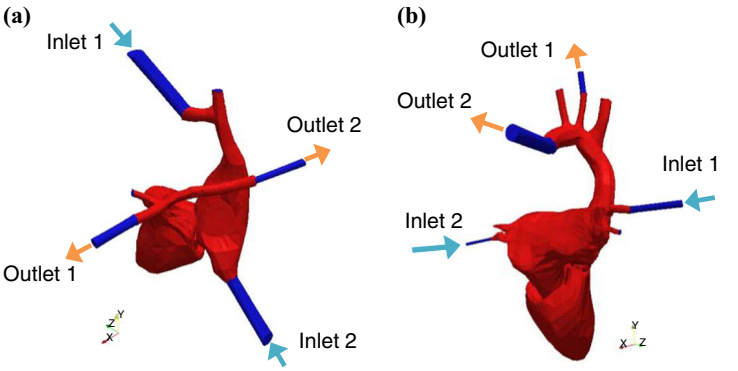

Figure 2.
Internal cooling system

Notes: (a) Coolant circulation directions for the right (pulmonic) heart; (b) coolant circulation directions for the left (systemic) heart

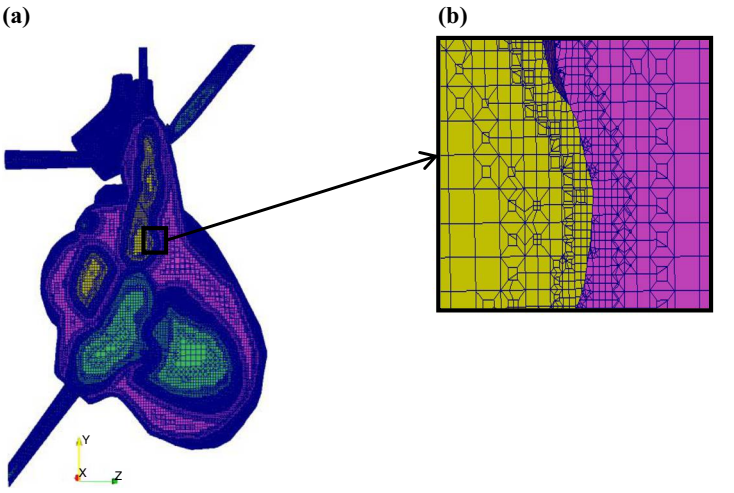

Figure 3.
Hexahedral mesh

Notes: (a) Heart, systemic and pulmonic domains (sagittal view); (b) enlarged view of a selected region

view. Heart's mesh in this figure is shown in pink, pulmonic domain's mesh in green and systemic domain's mesh in yellow. Figure 3(b) illustrates the mesh near the fluid-solid interface. The number of near-wall layers varied from 5 to 10 depending on the flow pattern. Mesh independency analysis was performed for all cooling cases by increasing the number of computational cells and mesh refinements. The total number of cells was increased from 5.4 million to 11 million. Results at 20 s showed the maximum error of 3.1 percent for the mesh with 5.4 million cells compared to the finer mesh. Therefore, this mesh was used for simulation of the rest of the cooling time period, in order to decrease the computing time.

6. Steady inlet velocities with two inlets for external circulation

The main objective of simulating the first heart cooling case, was to study effects of turbulent flow regime in enhancing heat transfer from the heart placed in a cooling container with two inlets and two outlets on the side walls. In the present analysis, the inlet vein flow velocity for the right heart pulmonary circulation was assumed to be 1.0 and 0.4 m/s for the left heart systemic circulation. Therefore, the values of Reynolds numbers at the inlets, with consideration of their diameters, are 1,662 and 1,773 for the right heart pulmonary circulation and 1,330 and 665 for the left heart systemic circulation. Considering these very low Reynolds numbers, the UW liquid flow inside the heart chambers and vessels was assumed to be laminar (Abdoli *et al.*, 2014a, b). The inlet velocity of the UW liquid for the external circulation was set to 1 m/s. The value of the Reynolds number at inlets of the external circulation domain was 4,155, indicated that the flow regime external to the heart was turbulent.

Figure 4 shows the calculated external flow streamlines with velocity and temperature distributions at 5 min with coolant inlet temperature at +4°C. As Figure 4 (a) illustrates, the maximum velocity of coolant was 1 m/s, which was located at the inlet. Figure 4(b) shows that the maximum temperature of the UW solution around the heart was +5.92°C.

Figure 5 shows calculated velocity and temperature distributions of the UW solution streamlines inside the heart pulmonary and systemic circulatory domains. Figure 5(a) illustrates that maximum velocity was 2.25 m/s. It occurred in the pulmonary circulatory domain, right after pulmonary semilunar valve. Figure 5(b) shows that maximum temperature variation of the UW solution inside the heart was +7.59°C. The coolant

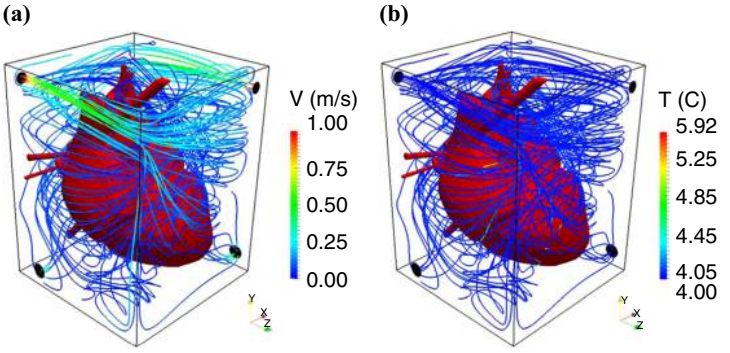

Notes: (a) Temperature distribution; (b) velocity distribution at five minutes

Figure 4.
Case 1 – UW coolant streamlines of external circulation

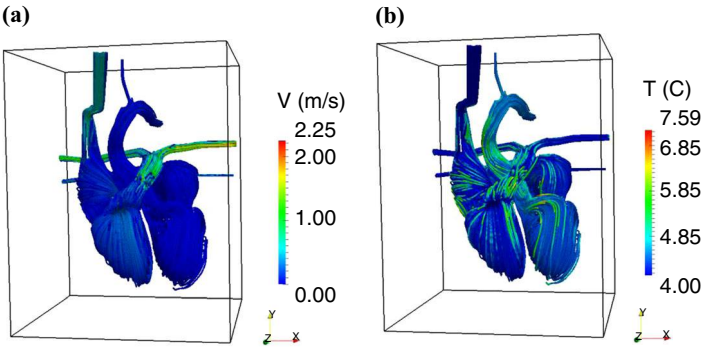

Figure 5.
Case 1 – UW fluid streamlines showing internal circulation

Notes: (a) Temperature distribution; (b) velocity distribution at five minutes

temperature in systemic circulatory domain was higher than the coolant temperature in the pulmonary circulatory domain. This was because of the lower velocity of the UW solution in the systemic circulatory domain than the pulmonary circulatory domain which can be observed in Figure 5(a). The lower coolant velocity increased the heat transfer interval between the coolant and the heart, and therefore increased the coolant temperature, thus enhancing the amount of heat removed from the interior of the heart. However, lower velocities in systemic circulation domain decreased the rate of heat removed by the coolant. In this research, effects of inlet velocity on heat transfer from the heart were investigated for the external and internal coolant flows.

Figure 6 shows translucent images of the calculated temperature variations within the heart at four different time instances using a constant color bar. As this figure illustrates, after 25 min of cooling, temperature in almost all parts of the heart was decreased to +5°C. To further study this cooling case, variations of the maximum, minimum and average volumetric temperatures of the heart tissue are shown in Figure 7(a). The average volumetric temperature refers to the average temperature of all computational cells considering their volume. It can be seen that the major reduction in the average volumetric temperature occurred within 25 min of cooling. The minimum temperature reached +4°C within a few seconds of cooling. This occurred as the coolant started flowing and touching the heart surface. The maximum temperature of the heart at 25 min was +12°C and at 60 min it was +4.5°C. Figure 7(b)

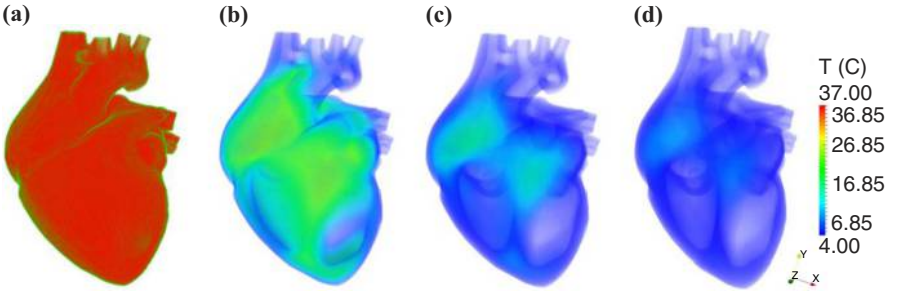

Figure 6.
Case 1 – temperature distribution of the heart tissue with constant color legend

Notes: (a) 0 min; (b) 5 min; (c) 15 min; (d) 25 min

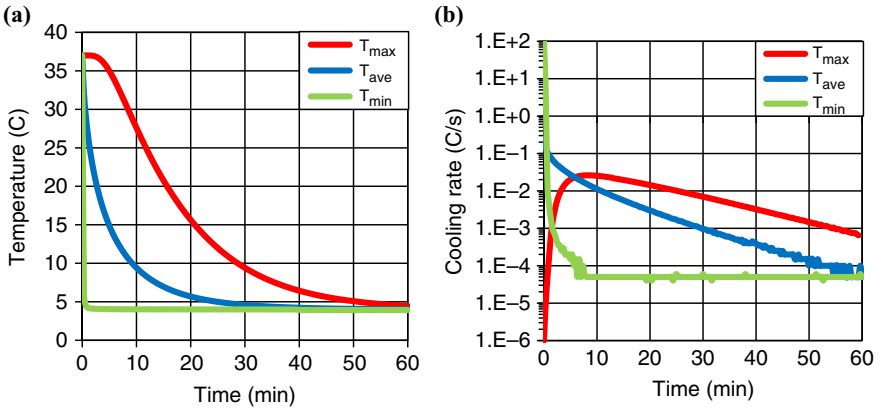

Figure 7.
Case 1 – temperature and cooling rate variations

Notes: (a) Maximum, minimum and average volumetric temperature inside the heart vs time; (b) cooling rate vs time (logarithmic scale)

illustrates the variation in cooling rates vs time for the maximum, minimum and the average volumetric temperatures of heart shown on a logarithmic scale. This figure shows that cooling rate for average volume temperature (T_{ave}) started at 0.247°C/s and gradually decreased to 0.0017°C/s at 25 min and to 5.0E−5°C/s at 60 min. The cooling rate for the minimum temperature was very high initially (31.1°C/s), but decreased rapidly after a few seconds and reached 0.001°C/s after 6 min. The maximum temperature started to decrease with an almost zero cooling rate, i.e., it did not cool at the beginning. Then, the cooling rate of the maximum temperature started to increase gradually and reached its maximum value of 0.0261°C/s at 8 min.

The CV of volumetric temperature (Equation (5)) is shown in Figure 8. The maximal value of CV was 1.45E−04, which occurred at 4 min. As this figure demonstrates, the non-uniformity of volumetric temperature increased until 4 min and then started to decrease gradually to 3.41E−5 at 25 min and to 1.77E−6 at 60 min. Therefore, the non-uniformity was decreased 4.25 times at 25 min compared to its maximum at 4 min. At 60 min the maximum non-uniformity was decreased to 81.92 times less than its maximum. Rate of metabolic rate was calculated by using Equation (1). The percentage of this metabolic rate reduction is shown in Figure 8(b) demonstrating that after 7.5 min of cooling, metabolic rate was reduced by 90 percent assuming that $Q_{10} = 2.5$. Then, the

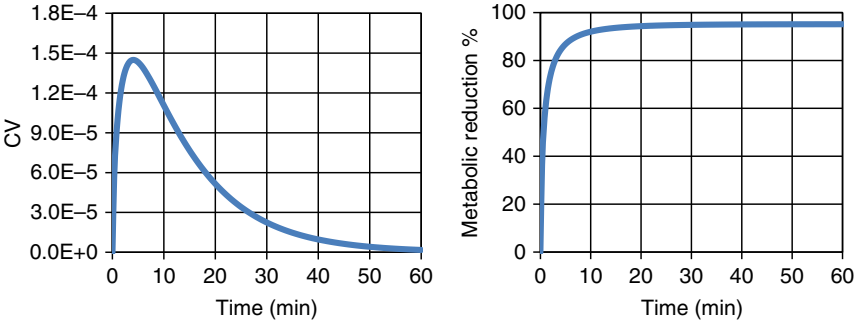

Figure 8.
Case 1 – coefficient of variation of volumetric temperature vs time (left) and percentage of metabolic rate reduction vs time (right)

reduction rate of metabolic rate slowed down rapidly. The metabolic rate reduction at 17 min was at 94.02 percent. Variations of metabolic rate reduction after 17 min were almost negligible.

In the next step, the stress analysis was performed by using the data obtained by the conjugate thermo-fluid analysis results. Normal and shear forces applied by the coolant flowing to the innermost and outermost surfaces were used as the boundary conditions on these surfaces. These values were updated for each physical time step. The heart temperature field was used to obtain the thermal stresses during the cooling process. The maximum von Mises stress is shown in Figure 9. The ultimate tensile stress of cardiac muscle is 110 kPa. As this figure demonstrates, the calculated von Mises stress has slight fluctuations around 100 kPa. The maximum value of von Mises stress was 103.67 kPa at 30 min. This shows that the effect of thermal stresses was not significant due to the very small Young's elastic modulus and thermal expansion coefficient of the heart tissue. Thus, only the shear forces caused by the flowing coolant played a major role in the stress field. The similar results were also reported by Abdoli *et al.* (2014a, b).

7. Case 2: steady inlet velocities with three inlets for external circulation

The main objective in this case was to place an additional inlet on the container wall creating a coolant jet flow right on the external surface of the heart where the hot spot was detected in Case 1, and study its effects in cooling the hot spot of the heart tissue. A jet flow will increase the convection heat transfer coefficient of the coolant flow around the heart. Figure 10 shows the new arrangement of nozzles on the walls of the cooling container with three inlets and two outlets for external circulation. Inlet 3 (Figure 10(b)) was designed so that it creates a jet on the external surface of the hot spot located above the right ventricle and on the right side of the right atrium.

Streamlines of the UW fluid with velocity and temperature distributions shown in color are depicted in Figure 11. Three jet flows can be seen in Figure 11(a). The maximum velocity of 1.04 m/s occurred right at the outlets. This was more than the inlet velocity of 1 m/s due to the extra inlet (inlet 3) which increased the total mass flow rate. Thus, the velocity of coolant at the outlets increased to satisfy the conservation of mass law.

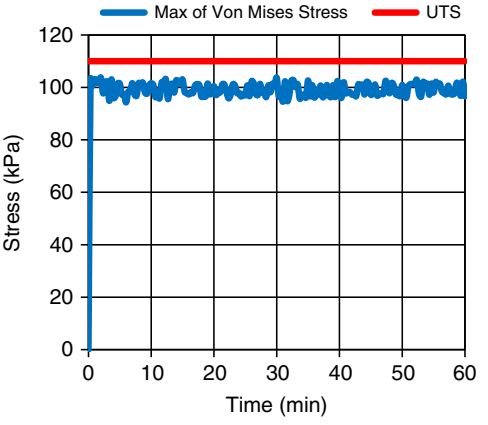

Figure 9.
Case 1 – maximum von Mises stress inside the heart and ultimate tensile stresses vs time

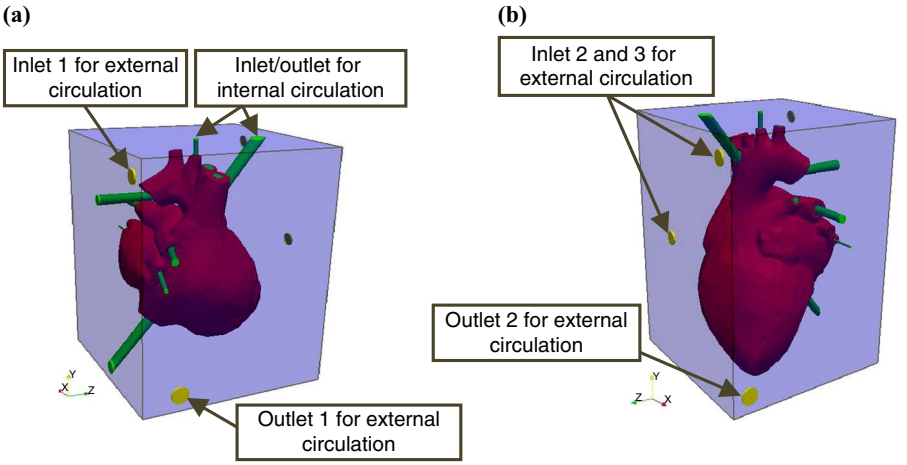

Notes: (a) Inlet 1 and outlet 1; (b) inlet 2, inlet 3 and outlet 2 for external cooling

Figure 10.
Case 2 – external cooling system

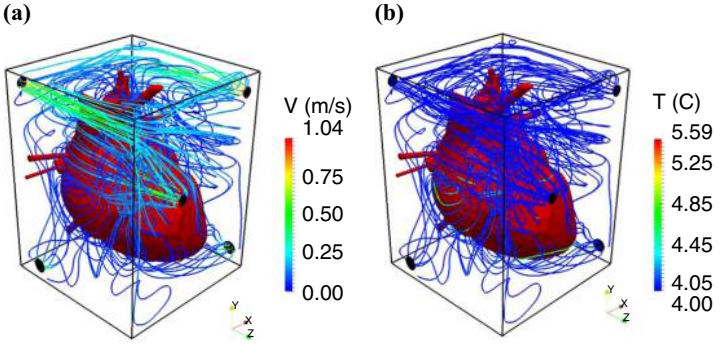

Notes: (a) Temperature distribution; (b) velocity distribution

Figure 11.
Case 2 – UW coolant streamlines for external circulation having 3 inlets and 2 outlets

To better illustrate the cooling jet flow at the hot spot, the heart model and UW coolant streamlines were cut at the hot spot. Color of heart in Figure 12(a)-(b) indicates the temperature field inside the heart at 5 min. Figure 12(a) clearly shows the jet flow on the external surface of the hot spot. In Figure 12(b), streamlines on the external surface of hot spot are not distinguishable due to negligible temperature difference between the heart external surface and the UW coolant streamlines.

Streamlines of the flows inside the heart pulmonary and systemic circulatory domains are shown in Figure 13. Boundary conditions for internal flow remained the same as in Case 1. Therefore, velocity and temperature distributions of the UW coolant within the heart in Case 2 were almost the same as in Case 1.

Figure 14 demonstrates the evolution of maximum, minimum and average volumetric temperature and their cooling rates during 60 min of cooling. It is apparent that there was no significant enhancement in cooling of the heart using the case with one extra inlet on the container wall. The results obtained for temperature

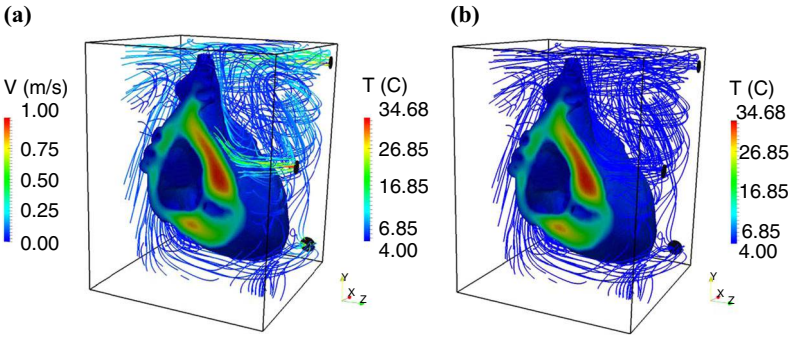

Figure 12.
Case 2 – cut-away of the external streamlines and the heart tissue showing

Notes: (a) Temperature field with a hot spot; (b) velocity field at five minutes

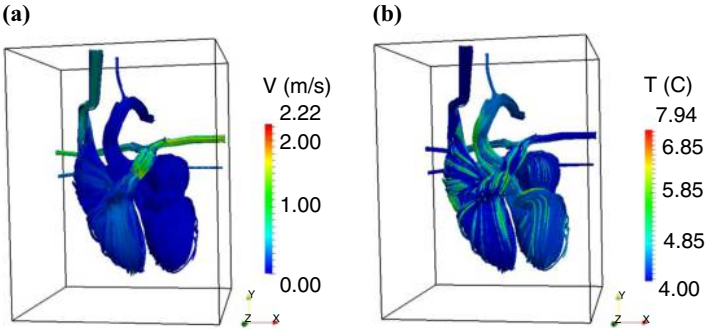

Figure 13.
Case 2 – UW coolant streamlines for internal circulation

Notes: (a) Temperature distribution; (b) velocity distribution

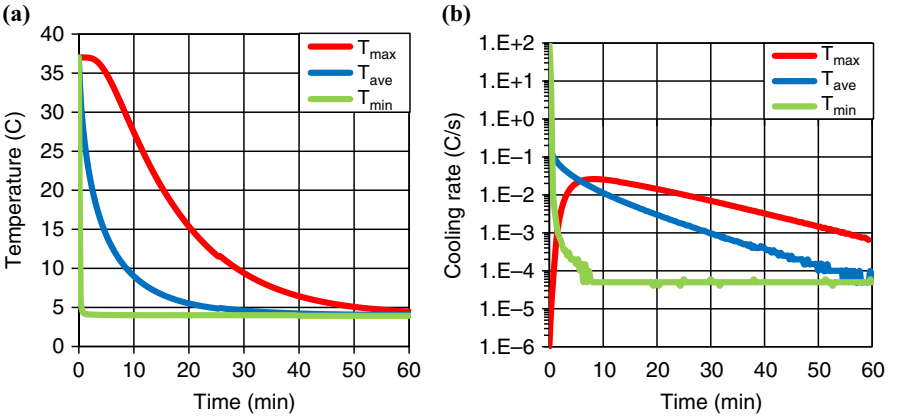

Figure 14.
Case 2 – temperature and cooling rate variations

Notes: (a) Maximum, minimum and average volumetric temperature inside the heart vs time; (b) cooling rate vs time (logarithmic scale)

non-uniformity and metabolic reduction rate were almost the same as those for the first case with two inlets on the walls. The reason for such results is discussed separately in Section 9.

8. Cases 3 and 4: unsteady inlet velocities with four inlets for external circulation

The aim of this section was to study effects of unsteady periodic inlet velocities on cooling of the heart. A cooling container with four inlets and four outlets was designed for simulations presented in this section. The reason for additional inlets in these cases was to examine the effect of higher coolant flow rates on cooling of the heart. Each of the four side walls had one inlet at its top right corner and one outlet at its bottom left corner. Figure 15 shows positions of inlets and outlets. Diameters of inlets and outlets were kept the same as in the previous cooling designs.

For unsteady periodic inlet velocities a sine function was used as follows:

$$V_{in} = V_0 + V_0 \sin(2\pi f t) \tag{13}$$

where f is the frequency and V_0 is the magnitude of inlet velocity. The average magnitudes of inlet velocities for the internal and external circulations were kept here the same as those in previous cases. Two relatively high frequencies (1 and 2 Hz) were chosen to study the flow frequency effect on the heart cooling. Figure 16 shows inlet velocity profile for the two unsteady cooling cases, where inlet velocity magnitude was 1 m/s ($V_0 = 1$ m/s). For such inlets, the maximum and minimum velocities were 2 and 0 m/s, respectively. As this figure illustrates, during a time period of 1 s, the inlet velocity in Case 3 had one complete cycle. For Case 4, inlet velocity had two complete cycles per 1 s period.

The maximum inlet Re numbers in Case 3 and Case 4 were double those in previous cases. Thus, the flow pattern for both internal and external circulations was assumed to be turbulent. Simulation results of unsteady cases, Case 3 and Case 4 are presented separately in the following two sections. Based on the results of Case 1 and Case 2, it can be concluded that the major reduction in the average volumetric temperature of the

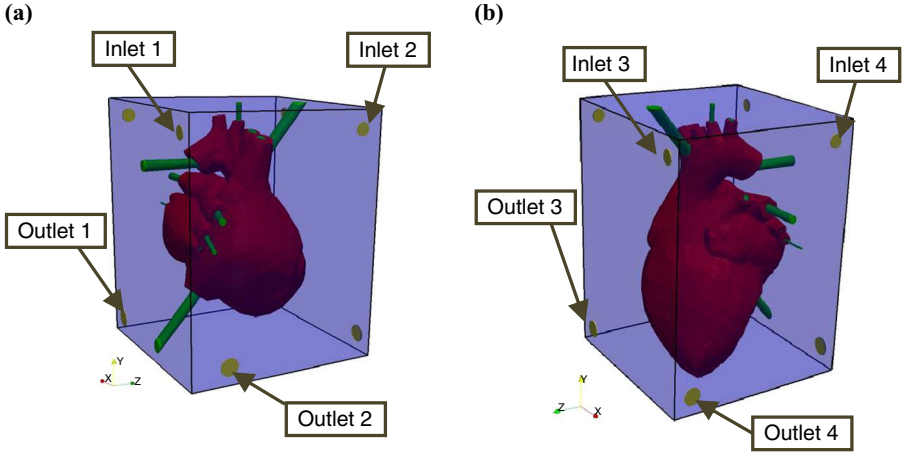

Figure 15. External cooling system

Notes: (a) Inlet 1-2 and outlet 1-2; (b) inlet 3-4 and outlet 3-4 for external cooling

heart occurred within 25 min of cooling. For this reason, unsteady Case 3 and Case 4 were simulated for 25 min. Results of these two cases did not show a significant enhancement compared to Case 1. A detailed comparison of all four cases is presented in the next section.

9. Discussion

Four heart cooling cases were numerically simulated in this study. The UW liquid was used for both internal and external coolant flow circulations. Abdoli *et al.* (2014a, b) numerically investigated the heart cooling process by using the UW liquid circulation within the heart and cooling gelatin from the outside of the heart for 25 min. In this study, the same heart geometric model was used for simulations. Table II shows the computational results of all cases at 25 min. Abdoli *et al.* (2014a) reported that after 25 min of cooling, the average volumetric temperature of the heart tissue reached +8°C. Results of the first case presented in this study indicated that the average volumetric temperature of the heart tissue decreased to +5°C at 25 min, which is 37.5 percent improvement. Abdoli *et al.* (2014b) reported an 18.9°C reduction of the maximum temperature of the heart tissue after 25 min of cooling that is from +37 to +18.1°C. The maximum temperature for the Case 1 in the present study was reduced to +12.0°C at 25 min, which shows 33.7 percent enhancement.

In Case 2, a hot spot inside the heart tissue was targeted with an additional cooling steady jet flow to examine its effects on improving the temperature uniformity. A jet flow of the UW coolant was created right on the external surface of the hot spot located above the right ventricle, and on the right side of the right atrium. The results showed that increasing h_{conv} at hot spots will not produce a significant difference in heat transfer from the hot spot. Case 3 and Case 4 had four inlets on cooling container side walls for the external circulation of the cooling liquid. Also, unsteady periodic boundary conditions

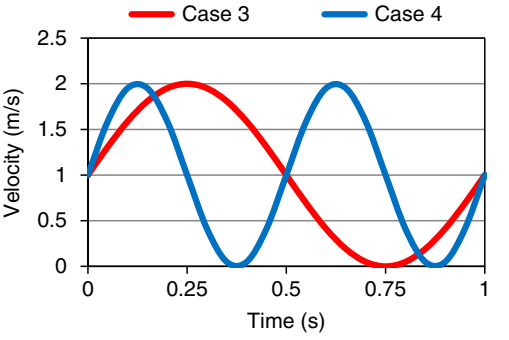

Figure 16.
Inlet velocity profile for Case 3 and Case 4 vs time ($V_0 = 1$ m/s)

Parameter	Steady Case 1	Steady Case 2	Unsteady Case 3	Unsteady Case 4	UW inside and gelatin outside
Minimum temperature (°C)	4.0	4.0	4.0	4.0	2.8
Maximum temperature (°C)	12.0	11.9	11.7	11.7	18.1
Average volumetric temperature (°C)	5.0	4.9	4.9	4.9	8.0

Table II.
Results of all heart cooling cases at 25 min

were applied for inlet velocities to enhance h_{conv}. However, almost the same results were obtained as in Case 1. This can be explained using the heat convection law:

$$q_{conv} = h_{conv} A\left(T_s - T_f\right) \tag{13}$$

Here, h_{conv} is the convection heat transfer coefficient, A is the contact area between fluid and solid surfaces. Based on this law, by increasing h_{conv}, convection heat transfer, q_{conv}, will increase in cases where A, T_s and T_f remain constant. By adding the third inlet in Case 2, h_{conv} was enhanced in the region above the hot spot. This helped removing the heat faster from the heart at the beginning of the cooling when $T_s - T_f$ was larger. As cooling proceeded, the value of $T_s - T_f$ decreased rapidly. Thus, effect of h_{conv} was decreased drastically, and conduction heat transfer within the heart tissue became the major limiting factor in the cooling process.

In this research, a parallel computer with the Red Hat Enterprise Linux Server 6.2 OS and LSF scheduler was used for simulations. Thermo-fluid simulations were run on 16 Intel (Xeon E5-2680 2.7 GHz) based cores with 128 GB memory. Each processor had six physical cores, 12 threads and 48 GB memory. Total computing time for Case 1 was 601,230 s and for Case 2 was 602,012 s for 60 min of cooling. Case 3 and Case 4 required smaller time steps due to their unsteady inlet velocities. Also, for these two cases more iterations were needed at each time steps. Total computing time for Case 3 was 346,924, and for Case 4 was 411,145 for 25 min of simulation.

10. Conclusions

In this study, four cooling systems for human heart preservation were designed and investigated numerically. In the first cooling design, the heart was internally and externally cooled by the UW cooling liquid. The UW coolant was pumped steadily to the cooling container through two inlets designed on the cooling container walls, while it was simultaneously steadily pumped inside the heart through its major veins. Each of internal circulatory systems (pulmonary and systemic) had two inlets and two outlets. Three-dimensional, conjugate thermo-fluid simulation results showed the average volumetric temperature of the heart was decreased by +32°C, that was from +37 to +5°C. The major reduction in the metabolic rate for the second design occurred until 17.3 min, which was 94.02 percent assuming that $Q_{10} = 2.5$. The Case 2 cooling design had three inlets for the external circulation. The Case 3 and Case 4 cooling designs had four inlets with unsteady periodic inlet velocities (1 Hz for Case 3 and 2 Hz for Case 4) and four outlets on side walls of the cooling container. Computational results reveal that after 3 min of cooling, conduction heat transfer (thermal diffusivity of the heart tissue) became the major limiting factor in the cooling process. Therefore, the additional inlet for the external flow in Case 3 and unsteady periodic inlet velocities and additional inlets and outlets in Case 3 and Case 4 did not improve the speed and uniformity of the cooling process. In this case, finding the minimum flow rates for the coolant would help to decrease the shear stresses, required pumping power and total size of cooling package.

The number of inlets and outlets for internal circulation can be increased from two to three or four to enhance the heat transfer. The optimal number of inlets and outlets can be determined by an optimization study.

For future research, one should use a more detailed human heart geometry which includes coronary arteries and cardiac veins. This way the coolant can be perfused within these veins and help to cool the heat walls faster. Also, the use of a model which differentiates between heart tissues such as vascular, muscle and fat tissues is needed.

As the heart rate decreases, the diastolic Ca^{2+} continues to rise, so relaxation is markedly reduced. Moreover, emission of ROS/RNS increases as a function of cooling. The high Ca^{2+} and the ROS/RNS have negative effect on the heart, even though protection against IR injury is improved by hypothermia (Stowe and Camara, 2009). One could incorporate the Ca^{2+} and ROS/RNS temperature based equations into the thermo-fluid system of equations to monitor their variation based on temperature.

References

Abdoli, A., Dulikravich, G.S., Bajaj, C., Stowe, D.F. and Jahania, M.S. (2014a), "Multi-disciplinary analysis of cooling protocols for human heart destined for transplantation", in Massarotti, N., Nithiarasu, P. and Sarler, B. (Eds), *ThermaComp2014*, Lake Bled, Slovenia, June 2-4, pp. 159-163.

Abdoli, A., Dulikravich, G.S., Bajaj, C., Stowe, D.F. and Jahania, M.S. (2014b), "Human heart conjugate cooling simulation: unsteady thermo-fluid-stress analysis", *International Journal of Numerical Methods in Biomedical Engineering*, Vol. 30 No. 11, pp. 1372-1386.

Amini, A.A. and Prince, J.L. (2001), *Measurement of Cardiac Deformations from MRI: Physical and Mathematical Models*, 1st ed., ISBN-13: 978-1402002229, Springer.

Arunachalam, B.K., Millard, R.W., Kazmierczak, M.J., Rodriguez-Rilo, H.L. and Banerjee P.K. (2006), "Evaluation of thermal efficacy of hypothermic tissue preservation methods", *Cell Preservation Technology*, Vol. 4 No. 2, pp. 97-116.

Bajaj, C. and Goswami, S. (2008a), "Modeling cardiovascular anatomy from patient-specific imaging", in Tavares, J. and Jorge, R. (Eds), *Advances in Computational Vision and Medical Image Processing*, Chapter 1, Springer, pp. 1-28, ISBN: 978-1-4020-9085-1.

Bajaj, C. and Goswami, S. (2008b), "Multi-component heart reconstruction from volumetric imaging", *Proceedings of the ACM Solid and Physical Modeling Symposium*, Stony Brook, New York, NY, pp. 193-202, available at: http://doi.acm.org/10.1145/1364901.1364928

Dennis, B.H. and Dulikravich, G.S. (2000), "Determination of unsteady container temperatures during freezing of three-dimensional organs with constrained thermal stresses", in Tanaka, M. and Dulikravich, G.S. (Eds), *International Symposium on Inverse Problems In Engineering Mechanics – Isip'2k*, Elsevier Science Ltd., Amsterdam, Nagano, pp. 139-148.

Dulikravich, G.S. (1988), "Inverse design and active control concepts in strong unsteady heat conduction", *Appl. Mech. Rev.*, Vol. 41 No. 6, pp. 270-277.

Ferziger, J.H. and Peric, M. (2001), *Computational Methods for Fluid Dynamics*, 3rd ed., Springer-Verlag, Berlin Heidelberg.

Freitas, R.A. Jr (1999), *Nanomedicine, Volume I: Basic Capabilities*, Landes Bio-science, Georgetown, TX, ISBN-13: 978-1570596803.

Hetnarski, R.B. and Eslami, M.R. (2009), *Thermal Stresses – Advanced Theory and Applications* ISBN 978-1-4020-9246-6, Springer.

Hou, G., Wang, J. and Layton, A. (2012), "Numerical methods for fluid-structure interaction – a review", *Commun. Comput. Phys.*, Vol. 12 No. 2, pp. 337-377.

Jahania, M.S., Sanchez, J.A., Narayan, P., Lasley, R.D. and Mentzer, R.M. (1999), "Heart preservation for transplantation: principles and strategies", *Ann. Thorac. Surg*, Vol. 68 No. 5, pp. 1983-1987.

Jasak, H. (1996), "Error analysis and estimation for the finite volume method with applications to fluid flows", PhD thesis, Imperial College, London.

Moore, E.M., Nichol, A.D., Bernard, S.A. and Bellomo, R. (2011), "Therapeutic hypothermia: benefits, mechanisms and potential clinical applications in neurological, cardiac and kidney injury", *Int. J. Care Injured*, Vol. 42 No. 9, pp. 843-854.

Mühlbachera, F., Langera, F. and Mittermayera, C. (1999), "Preservation solutions for transplantation", *Transplantation Proceedings*, Vol. 31 No. 5, pp. 2069-2070.

Ohayon, J. and Chadwick, R.S. (1988), "Effects of collagen microstructure on the mechanics of the left ventricle", *Biophys J.*, Vol. 54 No. 6, pp. 1077-1088.

OpenCFD Ltd (2011), "OpenFOAM", available at: www.opencfd.co.uk /openfoam/

Palmeri, M.L. and Nightingale, K.R. (2004), "On the thermal effects associated with radiation force imaging of soft tissue", *IEEE Transactions on Ultrasonics, Ferroelectrics, and Frequency Control*, Vol. 51 No. 5, pp. 551-565.

Park, J. and Lakes, R.S. (2007), *Biomaterials: An Introduction*, 3rd ed., ISBN-13: 978-0387378794, Springer-Verlag, New York, NY.

Peltola, J. (2011), "Adaptation and validation of openfoam®cfd-solvers for nuclear safety related flow simulations", in Pättikangas, T., Brockmann, T., Siikonen, T., Toppila, T. and Brandt, T. (Eds), *SAFIR2010 Seminar, 17.5.2011*, CSC, Espoo, pp. 1-20.

Polderman, K.H. and Herold, I. (2009), "Mechanisms of action, physiological effects, and complications of hypothermia", *Critical Care Med.*, Vol. 37 No. S7, pp. S186-S202.

Reyes, A.B., Pendergast, J.S. and Yamazaki, S. (2008), "Mammalian peripheral circadian oscillators are temperature compensated", *J. Biol. Rhythms*, Vol. 23 No. 1, pp. 95-98.

Southard, J.H. and Belzer, F.O. (1995), "Organ preservation", *Annual Rev. Med.*, Vol. 46 No. 1, pp. 235-247.

Sterk, M. and Trobec, R. (2005), "Biomedical simulation of heat transfer in a human heart", *J. Chem. Inf. Model.*, Vol. 45 No. 6, pp. 1558-1563.

Stowe, D.F. and Camara, A.K. (2009), "Review mitochondrial reactive oxygen species production in excitable cells: modulators of mitochondrial and cell function", *Antioxid Redox Signal*, Vol. 11 No. 6, pp.1373-1414.

Stowe, D.F., Heisner, J.S., An, J.Z., Camara, A.K.S., Varadarajan, S.G., Novalija, E., Chen, Q. and Schelling, P. (2002), "Inhibition of Na+/H+ Exchange-1 isoform protects hearts reperfused after six hour cardioplegic cold storage", *J. Heart Lung Transpl.*, Vol. 21 No. 3, pp. 374-382.

Trunk, P., Gersak, B. and Trobec, R. (2003), "Topical cardiac cooling – computer simulation of myocardial temperature changes", *Computers in Biology and Medicine*, Vol. 33 No. 3, pp. 203-214.

Yamada, H. (1970), *Strength of Biological Materials*, ISBN-13: 978-0683093230, Williams & Wilkins, Baltimore.

Further reading

Colvin-Adams, M., Smith, J.M., Heubner, B.M., Skeans, M.A., Edwards, L.B., Waller, C., Snyder, J.J., Israni, A.K. and Kasiske, B.L. (2011), "OPTN/SRTR 2011 annual data report: heart", *American Journal of Transplantation*, Vol. 13 No. S1, pp. 119-148.

Bajaj, C., Goswami, S., Yu, Z., Zhang, Y., Bazilevs, Y. and Hughes, T. (2006), "Patient specific heart models from high resolution CT", in Tavares, J.M.R.S. and Jorge, R.M.N. (Eds), *CompIMAGE*, Coimbra, October 20-21.

Kisslo, J.A. and Adams, B.D. (1987), *Principles of Doppler Echocardiography and the Doppler Examination #1*, Ciba-Geigy, London.

Zhang, Y. and Bajaj, C. (2004), "Finite element meshing for cardiac analysis", ICES Technical Report 04-26, University of Texas at Austin, Austin, TX.